Mechanical Behaviour of Hai Duong Medium Sand in Triaxial Test And Its DEM Simulations

Nguyen Quang Tuan[1] and Heinz Konietzky[2]
[1,2]*TU Bergakademie Freiberg, Geotechnical Institute, Freiberg, Germany*
[1]*E-mail*: nqtuan@tlu.edu.vn

ABSTRACT: This paper presents mechanical characteristics of Hai Duong medium sand - sampled from Chi Linh, Hai Duong - obtained from some laboratory tests. This sand is a typical constructional soil material and widely used in Northern Provinces of Vietnam. Specimens, obtained from compaction tests, were remoulded with dry unit weight of 95% of maximum dry unit weight. The drained triaxial compression tests on these dense sand specimens were performed under different confining pressures. Numerical simulations of the triaxial tests were carried out using the three dimensional particle flow code (PFC^{3D}) with a non-linear contact model. Numerical results were directly compared with the corresponding laboratory test results. The simulations show, that the particle based code PFC^{3D} is able to capture the mechanical behaviour of medium dense sand. Peak strength and stiffness of the sand specimens were well reproduced by the use of spheres with a simple rolling resistance model. The simulations also reveal the influence of the microscopic parameters of the model on the macroscopic behaviour of the sand.

Keywords: DEM, Triaxial test, Sand.

1. INTRODUCTION

Sand used for constructional purposes in Hanoi and its neighbouring provinces is mostly of alluvial origin. Sand is normally exploited along the river system, for example the Red river, the Thai Binh river and some other rivers in northern plain of Vietnam. The medium sand in this region is one kind of material which can be used for many different purposes, i.e. as aggregates for concrete, as fill material for foundations or embankments due to its abundant availability and reasonable costs. Study of the mechanical behaviour of this kind of sand is essential for design and analysis of stability and deformation. Mechanical parameters such as Young’s modulus, shear modulus, Poisson’s ratio and the stress-strain relation are essential for geotechnical engineering. Our research focuses on the mechanical behaviour of medium sand collected in Hai Duong province, Vietnam. Basic tests, i.e. grain size analysis, oedometer compression test, standard compaction test and drained triaxial compression tests were carried out. Triaxial test results were used for back analysis to derive the numerical simulation parameters for further calculation.

Recent developments of numerical methods and hardware together with corresponding computer-aided software for stress and strain analysis have increased effectiveness in design and dimensioning of geotechnical structures. The behaviour of sand can be simulated well by continuum approaches using finite element or finite difference methods. Within these approaches, simulations are performed at a global scale based on continuum constitutive models. The selection of suitable constitutive models and its parameters is very challenging. A finite element based method was used to simulate the stress-strain behaviour observed during drained triaxial compression tests to investigate the stress state dependency of deformation properties of sand (Nam and Khiêm 2008, Nam et al. 2008) and (Nam and Thảo 2013). The results show, that the stress-strain relationship of the medium sand during drained triaxial compression tests can be reasonably well simulated with the Hardening Soil model. Nevertheless, the dilation behaviour is not considered. For some particular cases, where an insight of the sand behaviour at the micro scale is needed, the common constitutive models implemented in most commercial codes are not satisfactory. The discrete element approach is a good alternative, because this method involves simulation at the micro scale and allows the consideration of the sand as a system of individual grains.

This study has been performed as an extensional part of the former project ‘’Study on stress state dependency of deformation characteristics of Hai Phong sand and Hai Duong sand’’ performed by a research group at Thuy Loi University (TLU), which was formerly named Vietnam Water Resources University, (Nam et al., 2008). The main objective of this paper is to demonstrate the capability of the discrete element method to simulate the behaviour of the selected medium sand using simple shaped particles and a simple contact model. Three dimensional particle flow code PFC^{3D} was used to simulate the drained triaxial tests. The effect of micro-parameters on the global behaviour of sand was studied. To take into account the grain shape and grain roughness, particles were prevented from free rolling. The numerical results were quantitatively compared with the experimental data from triaxial tests performed by Nam et al. (2008).

2. MEDIUM SAND OF HAI DUONG

The sand material selected for this research was medium sand with gravel in yellow colour. The sand samples were collected in Chi Linh, Hai Duong province. This sand is called Hai Duong sand. This sand can be considered as typical medium sand used for construction purposes in the region of Red river delta. The grain size distribution was obtained from sieve analysis, as shown in Figure 1. Proctor compaction tests were done to determine the maximum dry density and the optimum water content. The compaction curve is shown in Figure 2.

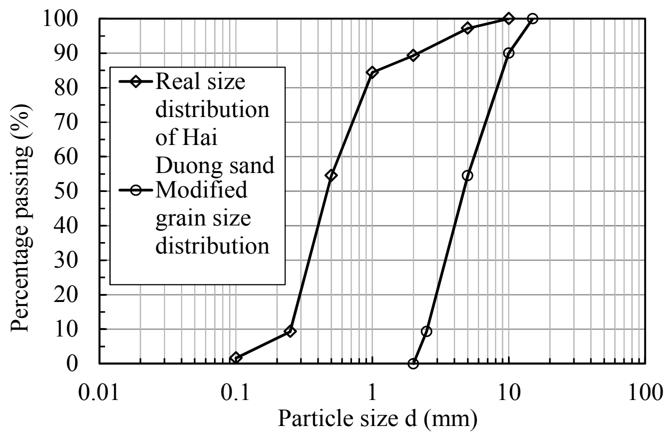

Figure 1 Grain size distribution of Hai Duong sand and modified curve for numerical simulation of triaxial test

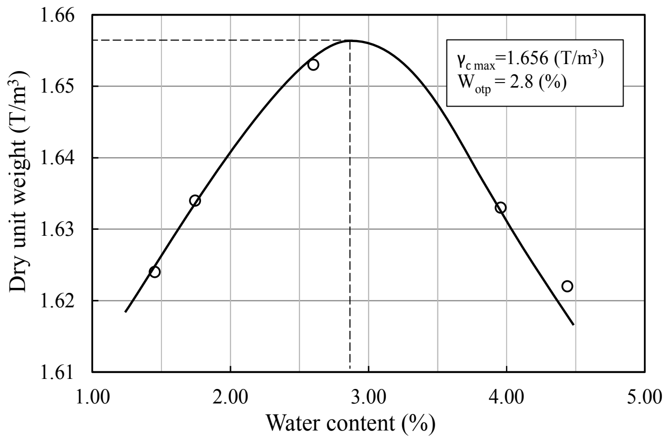

Figure 2 Compaction curve for Hai Duong sand

The triaxial tests were performed in the geotechnical laboratory of TLU. The triaxial compression tests were carried out under consolidated drained conditions. The testing procedure on specimen includes sample preparation, sample saturation, consolidation under drained conditions and finally loading up to failure. Detailed description of testing procedure was given by Nam et al. (2008).

Three sand specimens were prepared with water content maintained equivalent or close to its optimum value. The dry unit weight of specimen equals 95 percent of maximum dry unit weight (degree of compaction K = 0.95). This value of compaction degree is widely used in most of specifications or standards in Vietnam for common backfill applications. The dimensions of specimen are: 38 mm in diameter and 80 mm in height. Table 1 shows the basic properties of the tested material. Table 2 shows the properties of three sand specimens prepared for triaxial compression test.

The compression process of each sand specimen was started after cell pressure or confining pressure was applied and the consolidation was completed. Three levels of confining pressure, i.e. 100, 200 and 400 kPa, were selected for triaxial testing of sand. The duration of consolidation for each confining pressure was 6 hours. Then axial compression was increased under constant confining pressure until failure occurred. The results of triaxial compression tests show, that the relation between deviatoric stress and axial strain are obviously non-linear. The relation between volumetric strain and axial strain shows, that the volumetric deformation (dilation) increases with decreasing confining pressure. This behavior follows the general trend of sand as obtained by an earlier study of Duncan et al. (1980).

Table 1 Basic properties of Hai Duong sand

Property	**Value**
Specific gravity, G [-]	2.66
Maximum void ratio, e_{max} [-]	0.811
Minimum void ratio, e_{min} [-]	0.627
Maximum dry unit weight, γ_d [g/cm^3]	1.656
Optimum water content, W_{otp} [%]	2.8

Table 2 Properties of sand specimens prepared for triaxial compression tests

Specimen	Water content W (%)	Void ratio e	Porosity, n (%)	Dry unit weight (m^3)	Confining pressure (kPa)
HDA	5.05	0.691	40.86	1.573	100
HDB	5.03	0.694	40.97	1.57	200
HDC	5.01	0.690	40.83	1.574	400

3. DEM SIMULATIONS OF TRIAXIAL TESTS

The triaxial compression behaviour of sand via DEM has been studied by a number of researchers. Katzenbach and Schmitt (2004), and Kozicki et al. (2014) made relatively comprehensive studies on the application of three-dimensional DEM model to simulate triaxial compression test on sand. In their studies, grains were modelled by means of clumps or spheres with rolling resistance. The confining boundaries were rigid walls. The effects of grain size distribution and initial porosity of specimen were considered. Recently, Bono et al. (2012) and Mehmet and Alshibli (2014) developed a flexible membrane boundary for triaxial tests. This improves the simulation of the volumetric response but requires more computational effort. DEM models were also used for analysis of triaxial behaviour of gravel (Stahl and Konietzky 2011) and fibre-reinforced sand (Polak et al. 2015, Tuấn 2015, Wang and Leung 2008, Yamaguchi et al. 2009) or cement treated sand (Hamidi and Hooresfand 2013).

In this study, the numerical model was created with the same dimensions as the sand specimen tested in the lab, i.e. height of 80 mm and diameter of 38 mm. Porosity of the particle assembly and the particle size distribution are replicated in the numerical specimen. Some previous studies, e.g. by Katzenbach & Schmitt (2004), have shown that the grain size distribution has a strong effect on the stress strain behaviour. The ideal approach is to use the real grain size distribution of sand (1:1 simulation). Theoretically, any given grain size distribution can be simulated. However, in practice this often would lead to a huge number of particles, far beyond the limit of current software and computer capacity. Therefore, so-called ‘parallel grading’ is often used. This procedure is not practicable here, because scaling factor has to be smaller than 2 due to ratio between samples size and maximum particle diameter. Such small ‘parallel grading’ would lead to a final particle number of more than 1 Million particles. Besides, the wide range of particle size slow down the computational process, because the smallest particle determines the time step applied in DEM codes. Moreover, the time necessary to bring a model to equilibrium increases with the amount of particles in the model. Therefore, in order to simulate the problem effectively, the real grain size distribution of sand needs to be modified and up-scaled as shown in Figure 1. Because the grain sizes of Hai Duong sand vary quite strongly, the original grain size distribution was modified marginally by limiting the coarse size and rejecting the fine size before upscaling. Specifically, those parts at which the amount of finer or coarser size occupies less than 10 % were cut and the curve modified. The number of particles in the numerical specimen depends on the upscaling factor. Upscaling factor is used to enlarge all particles by multiplying their diameter by a certain value. An upscaling factor of 7.5 was used here, while the dimensions of the numerical specimen are exactly the same as the specimen dimensions used in the laboratory tests. A special algorithm was developed to calculate the number of particles for each size range.

3.1 Specimen preparation of numerical model

To conduct PFC^{3D} simulations, an assembly of particles has to be generated and microscopic particle and contact properties have to be assigned. At the begin spheres were shrunk to small sizes before placing at random positions inside the envelope of the specimen. In case of using particles of arbitrary shape, every sphere is replaced by a clump with the same volume, a new equivalent density and a random orientation. The particles were then expanded back to the desired final size in several steps. This method simplifies the placement of particles and reduces the overlap, which can cause initial high contact force inside the specimen. Friction of particles was set to zero to allow particles to move without sliding resistance.

The micro parameters (see Table 3) of the model were set at the begin of the simulations. In case of using spherical particles rotational movement of any particle was inhibited by setting the rotational velocity components to zero after specimen preparation and no-rolling-condition was kept while stepping. The reason for this treatment is, that in reality sand particles have irregular shape and specific surface texture, which leads to interlocking and substantial reduction of rolling capability. Fixing rotational velocity is the simplest way to resist the rolling of spherical particles. Different other techniques can be used instead, i.e. rolling resistance models at contacts, arbitrary particle shapes by using clumps or clusters (e.g. Stahl and Konietzky, 2011; Tuấn and Konietzky, 2013). However, these methods require calibration of parameters and more computational power.

Table 3 Parameters for numerical triaxial tests using Hertz contact model

Parameter	Value
Contact shear modulus, G_c (Pa)	1.0×10^8 to 10^9
Contact Poisson's ratio, ν_c (-)	0.001; 0.01; 0.1; 0.25; 0.45
Porosity of sample, n	0.41
Wall normal stiffness (N/m)	1.0×10^5
Wall shear stiffness (N/m)	0.0
Friction coefficient of contact	0.1 to 1.5
Friction coefficient of walls	0.0
Particle density (T/m^3)	2650

The use of the Hertz-Mindlin contact model, as described by Itasca (2008), demands the specification of the following input parameters: contact shear stiffness G_c, contact Poisson's ratio ν_c, contact friction coefficient μ. An extra parameter, called rolling resistance factor RF was added to control the rotational movement of spherical particles. Numerous researches have investigated the influence of the micro parameters on the macroscopic behaviour, which is characterized by different parameters such as peak and post failure strength, dilatancy angle ψ, secant stiffness modulus E_{50} and Poisson's ratio ν. It should be noted that the Poisson's ratio of soil specimen is different from the Poisson's ratio at contacts.

The models of triaxial sand specimen incl. boundaries are shown in Figure 3. Two flat walls at the top and the bottom of the generated specimen are used as loading platens. There are several methods to apply confining pressure, e.g. rigid flat boundaries, rigid cylindrical boundaries or flexible particle boundaries. In this research, cylindrical wall boundaries were chosen. A study was performed to compare the effects of single cylindrical boundary vs. multi cylindrical boundary as reported in section 3.4. Finally, the single cylindrical wall boundary was selected for the simulations presented within this paper.

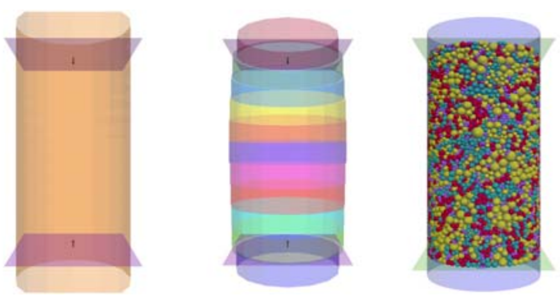

Figure 3 Geometry of models: (a) single-wall boundary; (b) multi-wall boundary (after test); (c) specimen filled with spheres

After specimen was prepared, final micro parameters were assigned to the model. The specimen was brought into equilibrium under a prescribed confining stress, i.e. isotropic stress state. This isotropic stress was introduced to the model by moving walls driven by a servo mechanism. All walls are frictionless, and the normal stiffness of the loading platens and the confining wall are set equal to one tenth of the particle contact stiffness. The servo mechanism is used to load the specimen in a stress-controlled manner. Different levels of confining pressure were applied simply by setting the required isotropic stress value and iterating the model until the required state was reached. Then, the specimen was additionally loaded in the vertical direction.

3.2 Numerical testing procedure

The triaxial test is performed in two stages: Isotropic loading stage and deviatoric loading stage. Macroscopic stresses and strains of the specimen are determined by computing the stresses and relative displacement of the opposite walls. The history logic is used to monitor the evolution of the system.

3.2.1 Isotropic loading stage

After the specimen is prepared, the servomechanism is activated, and walls are moved until the measured horizontal and vertical stresses are close to the required stresses.

3.2.2 Deviatoric loading stage

In this stage an equal and opposite constant velocity is applied to the upper and lower walls (loading platens), to perform a controlled compression test. The cylindrical walls are moved via the servo-control mechanism described previously to maintain the confining stress. Compression continues up to 10% vertical deformation.

3.3 Interpretation of simulation results

The model parameters were chosen by matching the experimental results with the numerical ones. Several attempts were made to evaluate the influence of the microscopic input parameters on the macroscopic stress-strain behaviour.

The macroscopic behaviour of sand specimen under triaxial compression is characterized by typical stress strain curves and corresponding macroscopic parameters as shown in Figure 4.

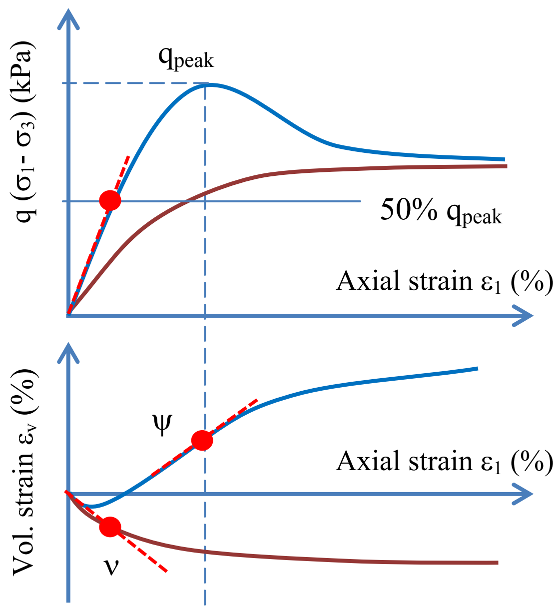

Figure 4 Typical behaviour and corresponding macroscopic parameters of sand under triaxial compression

Key parameters are (Figure 4):

- Peak deviatoric stress q^{peak} and residual deviatoric stress $q^{residual}$
- Stiffness modulus E_{50} (secant modulus)
- Poisson's ratio ν
- Dilatancy angle ψ

It is easy to match the part of the stress strain curve before failure. However, to fit the complete stress-deformation behaviour with all the nonlinearities including dilation and post failure behaviour is a quite challenging task.

3.4 Influence of confining methods

One important aspect in modelling triaxial tests is the method, how confining stress is applied to the sample. A number of different methods have been proposed, e.g. the use of multiple rigid cuboid walls (Belheine et al. 2009, Katzenbach and Schmitt 2004) or the use of particles at the outer boundary of the cylinder (Bono et al. 2012, Kozicki et al. 2014, Mehmet and Alshibli 2014, Wang and Leung 2008). In this research, a cylindrical servo-controlled wall was used to create the confining pressure. A more flexible boundary can be created by using a series of cylindrical walls instead of one single one. The servo mechanism is also assigned to these walls to maintain a required stress state. The radial bulging behaviour of specimen is captured more accurately. In a preliminary study, a series of 11 cylindrical segments were used as confining boundaries, see Figure 3(b). Due to the fact, that volumetric deformation in lab testing was recorded via burette readings, the multi-wall boundary was chosen. The radial strain of every segment was recorded to calculate the volumetric strain. It can be seen, that the secant modulii obtained from both models (single and flexible boundary type) are equal. Peak deviatoric stress and dilatancy are slightly smaller in the flexible model. However, the differences are not remarkable (Figure 5). Hence, single rigid wall was used as boundary condition for this study. However, in general flexible walls should be preferred.

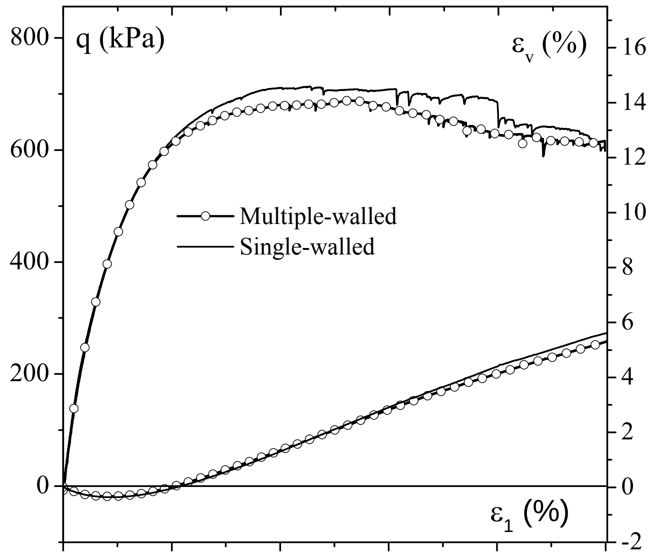

Figure 5 Macroscopic deviatoric stress q and volumetric strain versus axial strain of numerical triaxial tests comparing one-wall and multi-wall boundaries (no rolling, μ = 0.25, $G_c = 10^9$ MPa, ν_c = 0.25, σ_3=200 kPa)

3.5 Effects of microscopic parameters

3.5.1 Influence of contact stiffness

It was found that the confining wall stiffness has influence on the stress-strain behavior. Higher wall stiffness causes higher peak strength and higher apparent specimen stiffness. In this study, wall normal and shear stiffness of 10^5 Pa was used throughout all simulations.

The contact stiffness of Hertz-Mindlin model is characterized by contact shear modulus and contact Poisson's ratio. It was found that the shear modulus of the contact stiffness has significant influence on the compression behaviour. The elastic response is mainly governed by contact stiffness. Higher contact shear modulus results in higher peak strength and stiffer response, see Figure (6a). The influence of the contact shear modulus on the volumetric behaviour is illustrated in Figure 6(b) and shows that low values of contact shear modulus result in more pronounced dilation.

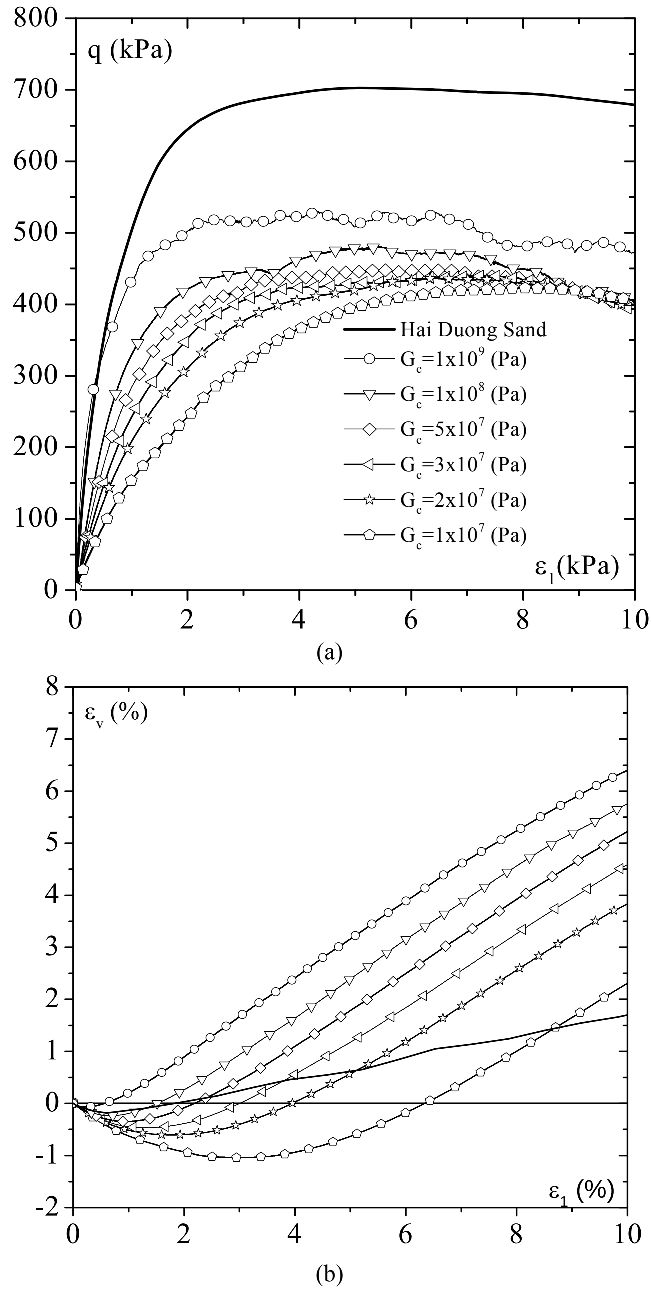

Figure 6 Macroscopic deviatoric stress (a) and volumetric strain (b) versus axial strain of numerical triaxial tests with different contact shear moduli G_c (μ = 0.3, ν_c = 0.25, σ_3=200 kPa)

The Figure 7(a) shows the relationship between macroscopic secant modulus E_{50} and the microscopic shear modulus for confining pressure of 200 kPa for different values of rolling resistance. It can be seen that the relationship is nonlinear. Except the case of no rolling resistance, the E_{50} is a power function of contact shear modulus with high correlation coefficient.

It is found that contact stiffness has a significant effect on the deformation characteristics and a small effect on the peak deviatoric stress. The contact stiffness has also a strong effect on the initial subtraction while it seems to have no influence on the dilation.

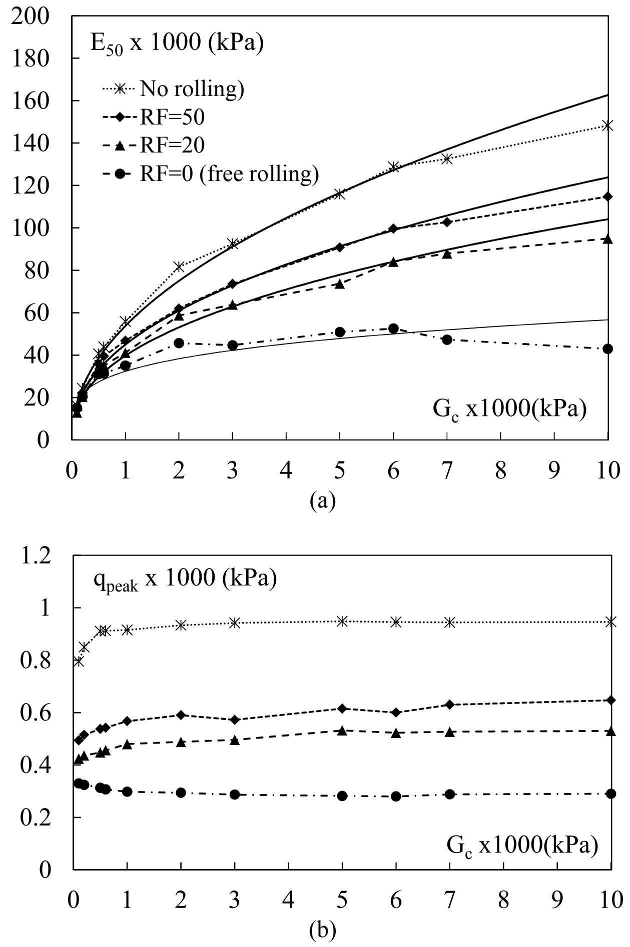

Figure 7 Relationship between (a) macroscopic secant stiffness modulus E_{50} with fitted power functions and (b) macroscopic deviatoric stress q_{peak} versus micro contact shear modulus G_c for different values of rolling resistance factor RF at a confining pressure of 200 kPa.

3.5.2 Influence of contact friction coefficient

Figure 8 shows that contact friction strongly influences both, the mobilized peak stress and the dilation. Increasing microscopic friction μ results in an increase of peak strength and dilation angle. Besides, it also has influence on the residual deviatoric stress. Increase of friction coefficient leads to a rapid decrease of stress in the post-peak region as shown in Figure 8.

Comparison of the simulation results with stress-strain curves of the lab tests leads to the conclusion, that a low contact friction angle should be used to get a satisfying agreement for both, dilation and post-peak behavior. The calculated maximum internal friction angle ϕ is dependent on inter-particle friction coefficient μ.

3.5.3 Influence of rolling resistance

Rolling resistance in this study is governed by an artificial restraining mechanism and parameterized by rolling resistance factor (RF), i.e. number of time-steps in which particles are prevented from rotation.

As expected, the results in Figure 9 show, that higher rolling resistance results in a stiffer response and higher strength. As also shown in Figure 9, the rolling resistance has smaller effect on the dilation behavior of the specimen. However, with high value of RF, the dilation varies in a very small range.

It was found, that beside microscopic friction of particles, the rolling resistance has significant influence on the peak stress of the numerical specimen. The joined effect of microscopic friction and rolling resistance on peak strength, which is characterized by the macroscopic friction angle, can be seen in Figure 10.

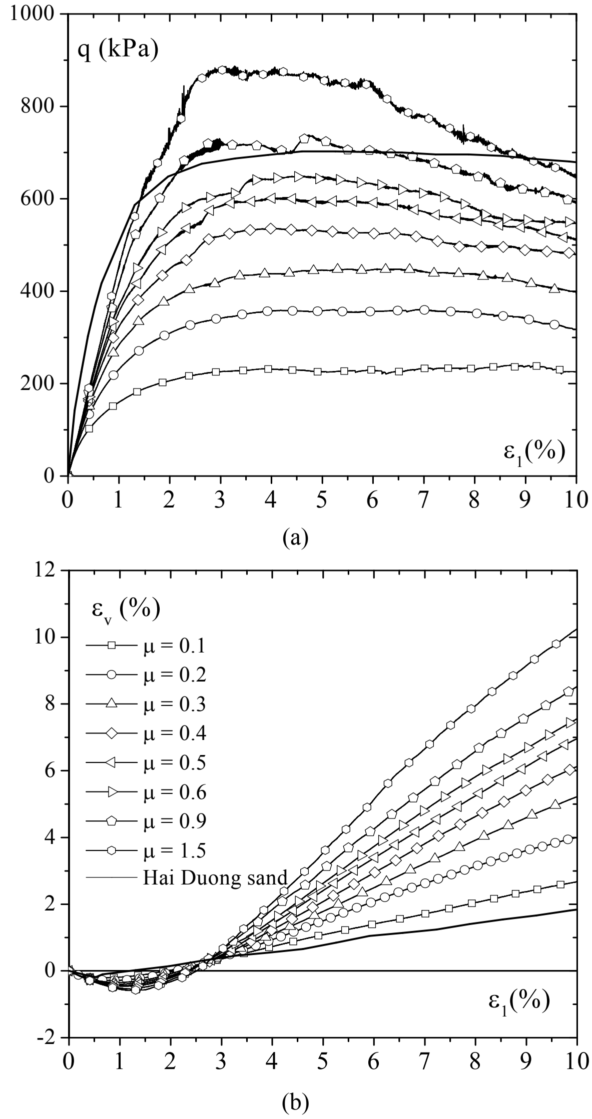

Figure 8 Macroscopic deviatoric stress (a) and volumetric strain (b) versus axial strain of numerical triaxial tests for different contact friction coefficients μ (G_c= 500MPa, ν_c=0.25, σ_3=200 kPa, RF=20)

3.6 Parameter calibration

Calibrations were performed to match the lab testing results. All three specimens with 3 levels of confining pressure were used for calibration. Results are illustrated together with lab results in the corresponding diagrams. Detailed validation using alternative lab tests, physical models or field tests were not yet performed. Because the influence of the micro parameters on the macroscopic behavior of the specimen is manifold, the calibration work was performed in several steps. First, contact shear stiffness G_c was varied to match the slope of the stress – strain curve. Because Poisson's ratio of contact has insignificant effect on the simulation results, a constant value of 0.25 was used. Then, contact friction coefficient was adjusted to match the dilation curve as close as possible. Finally, rolling resistance factor RF was adjusted to match the peak stress (Gao and Zhao 2013) .

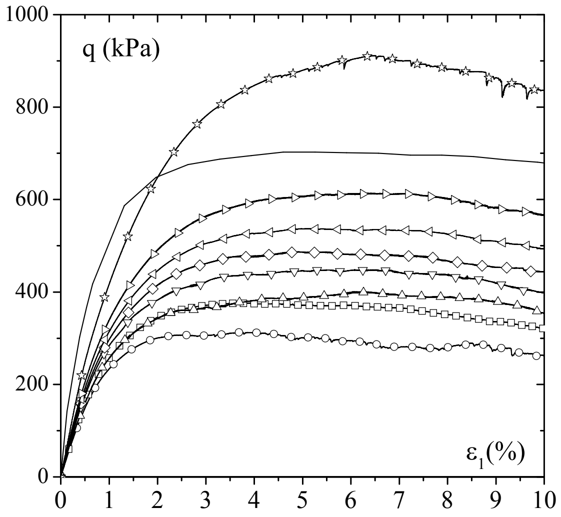

(a)

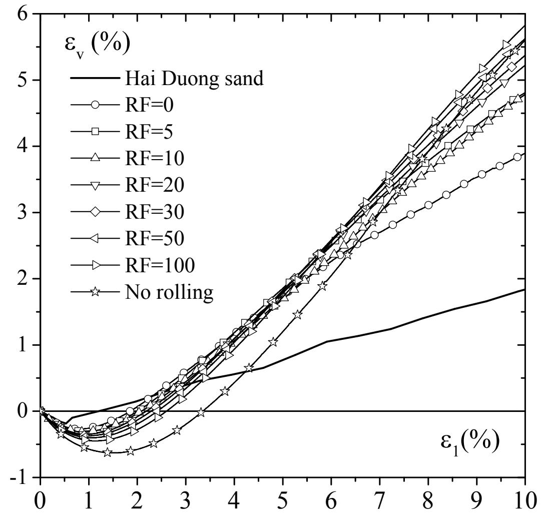

(b)

Figure 9 Macroscopic deviatoric stress versus axial strain (a) and volumetric strain versus axial strain (b) of numerical triaxial tests with different rolling resistance factors RF (μ = 0.3, G_c = 500 MPa, ν_c = 0.25, σ_3 = 200 kPa)

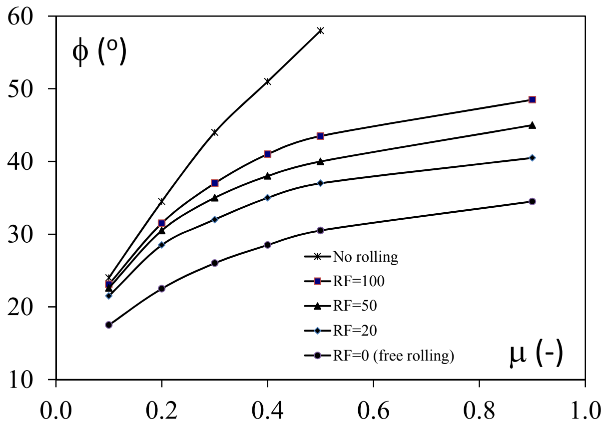

Figure 10 Relation between macroscopic friction angle ϕ and microscopic friction coefficient of particles with different values of rolling resistance factor RF (G_c= 500MPa, ν_c= 0.25, σ_3=200 kPa)

Figure 11 shows lab results together with simulation results obtained with the calibrated micro parameters given in Table 4 for confining pressures of 100, 200, 400 kPa. This comparison shows that the stress-strain behavior of sand is well reproduced although the dilation is over predicted by the numerical model. In the non-linear stress-strain relation the stiffness modulus continuously decreases until peak axial stress is reached. Thus, the stiffness modulus value is dependent on both, the contact stiffness and the contact friction coefficient. The peak value depends on the contact friction assigned to the particles.

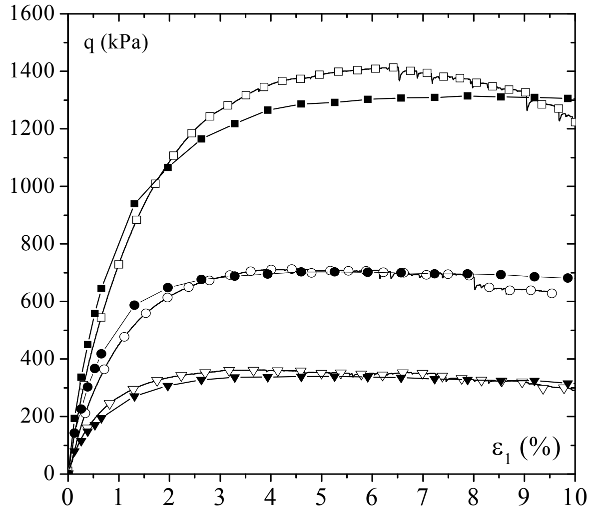

(a)

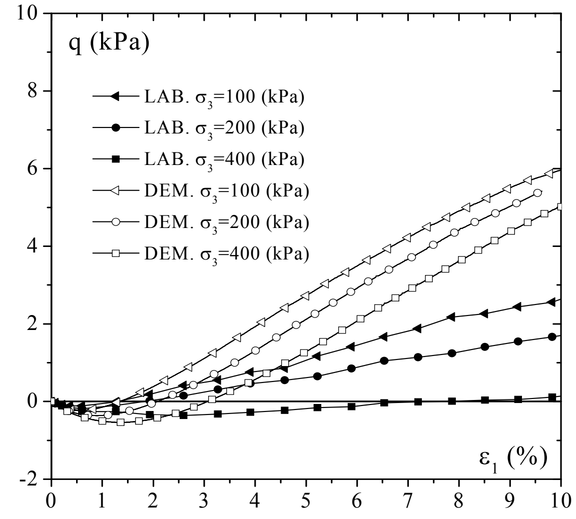

(b)

Figure 11 Deviatoric stress and volumetric strain versus axial strain for the laboratory triaxial tests of Hai Duong sand and numerical simulations

Table 4 Values of calibrated parameters for numerical model

Parameter	Value
Contact shear modulus, G_c [Pa]	1.0×10^9
Contact Poisson's ratio, ν_c [-]	0.25
Wall normal stiffness [N/m]	1.0×10^5
Wall shear stiffness [N/m]	1.0×10^5
Friction coefficient of contact	0.25
Friction coefficient of walls	0.0
Rolling resistance	No rolling

It was also found from Katzenbach and Schmitt (2004) and Hainbüchner et al. (2002) that the upscale factor of grain size used in numerical models has minor influence on stress-strain curves, but can overestimate the dilation.

Based on simulation results, Mohr circles and the linear failure envelope were constructed for peak stresses. Figure 12 shows a comparison between simulated and experimental failure envelopes. Since no cohesion exists, the failure envelope intercept with the origin. Macroscopic friction angles were obtained as shown in Figure 13. The slope of the failure envelope gives a macroscopic friction angle. A maximum macroscopic friction angle of 39.5 degrees was obtained corresponding to the applied microscopic friction coefficient of 0.25.

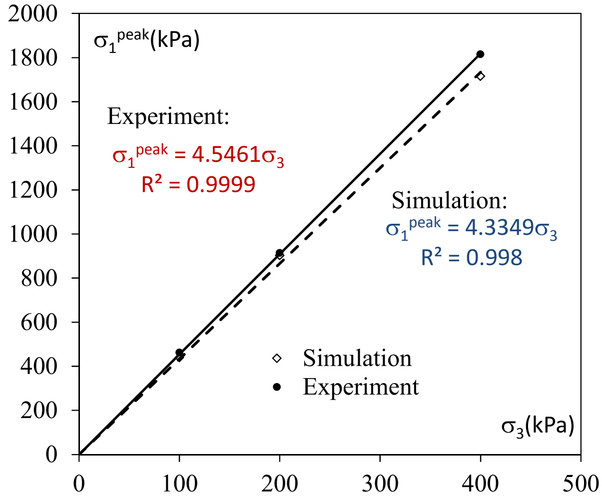

Figure 12 Principal stresses at failure obtained from laboratory experiments and numerical simulations for different confining stresses

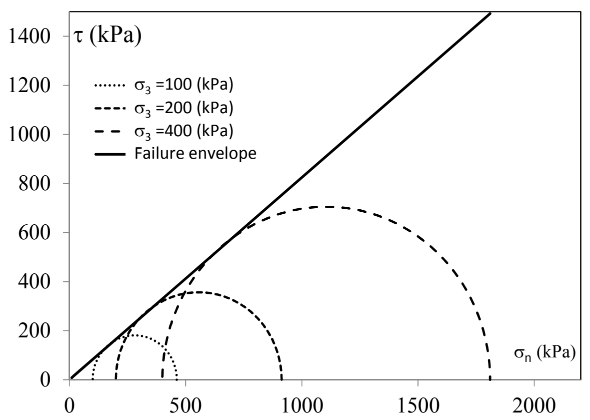

Figure 13 Failure envelope deduced from numerical simulations on Hai Duong sand

4. CONCLUSIONS

The mechanical behaviour of Hai Duong sand under triaxial loading conditions has been simulated using discrete numerical models. It is found that spherical particles can be used to produce stress-strain behaviour observed in the lab, if simple rolling resistance scheme is applied. From a series of numerical simulations at different stress levels, the stress state dependency of deformation pattern was found. The macroscopic behavior characterized by nonlinear stiffness, contraction, dilation and peak strength can be captured by the DEM.

Grain shape and surface roughness of sand grain can be covered by means of simple rolling resistance. By using this simple method only four micro-mechanical parameters are needed: contact shear modulus, contact Poisson's ratio, contact particle friction coefficient and rolling resistant factor. Those can be calibrated on the basis of triaxial lab tests.

The peak macroscopic friction angle is governed by the microscopic parameter μ. The dilation of specimens is rather overestimated by DEM, possibly due to the effect of upscaling the particle size and the fact, that lab measurements are of questionable quality.

The higher the confining pressure, the smaller are both, the global friction and the dilatancy angle.

The relations between micro and macro parameters were established, especially the relation between microscopic shear modulus G_c and macroscopic secant modulus E_{50}. Also, the combined relation between microscopic friction coefficient μ accompanied with rolling resistance factor RF and the macroscopic friction angle of sand.

The stress-strain behaviour of Hai Duong sand in triaxial tests is well reproduced by the numerical model. Nevertheless, intensive validation is necessary as next step.

5. ACKNOWLEDGMENTS

The work presented in this paper is an extension to the research project ''Study on stress state dependency of deformation characteristics of Hai Phong sand and Hai Duong sand'', which was supported by Thuyloi University. The authors thank the board of the financial support and the research group. Thanks also to the anonymous reviewers for valuable hints to improve the quality of the paper.

6. REFERENCES

Belheine, N., J. P. Plassiard, F. V. Donzé, F. Darve & A. Seridi, 2009. Numerical simulation of drained triaxial test using 3D discrete element modeling. Computers and Geotechnics 36: 320-331.

Bono, J. D., G. Mcdowell & D. Wanatowski, 2012. Discrete element modelling of a flexible membrane for triaxial testing of granular material at high pressures, pp. 199-203 in Géotechnique Letters.

Duncan, J. M., P. Byrne, K. S. Wong & P. Mabry, 1980. Strength, Stress-Strain and Bulk Modulus Parameters for Finite Element Analysis of Stress and Movements in Soil Masses, pp. University of California, Berkeley.

Gao, Z., & J. Zhao, 2013. Evaluation on failure of fiber-reinforced sand. Journal of Geotechnical and Geoenvironmental Engineering 139: 95-106.

Hainbüchner, E., Potthoff, S, Konietzky, H. & te Kamp, L., 2002. Particle based modeling of shear box tests and stability problems for shallow foundations in sand, in: Numerical Modeling in Micromechanics via Particle Methods (Ed. H. Konietzky), A.A. Bakema

Hamidi A, Hooresfand M. 2013. Effect of fiber reinforcement on triaxial shear behavior of cement treated sand. Geotextiles and Geomembranes 36: 1-9.

ITASCA, 2008. PFC3D Version 4.0 - Theory and Background. Itasca Consulting Group, Inc., Minneapolis, Minnesota.

Katzenbach, R. & A. Schmitt, 2004. Micromechanical modeling of granular materials under triaxial and oedometric loading, pp. 313 - 322 in Numerical Modeling in Micromechanics via Particle Methods - 2004: Proceedings of the 2nd International PFC Symposium, edited by Y. SHIMIZU, R. HART and P. CUNDALL. Routledge, Kyoto, Japan.

Kozicki, J., J. Tejchman & H.-B. Mühlhaus, 2014. Discrete simulations of a triaxial compression test for sand by DEM. International Journal for Numerical and Analytical Methods in Geomechanics 38: 1923-1952.

Mehmet, B. C., & A. K. Alshibli, 2014. 3D analysis of kinematic behavior of granular materials in triaxial testing using DEM

with flexible membrane boundary. Acta Geotechnica 9: 287-298.
Nam NH, Khiêm NĐ. 2008. Nghiên cứu sự phụ thuộc trạng thái ứng suất của các đặc tính biến dạng của cát hải phòng và cát hải dương. Tạp chí khoa học kỹ thuật Thuỷ lợi và Môi trường, Trường Đại Học Thuỷ Lợi: 62-70.
Nam NH, Mẫn NC, Tuấn NQ, Khiêm NĐ. 2008. Nghiên cứu sự phụ thuộc trạng thái ứng suất của các đặc tính biến dạng của đất cát trong thiết kế tường chắn đất. Hanoi: Hanoi Water Resources University. Research Report.
Nam NH, Thảo NP. 2013. Effect of soil models on the deformation and pressures on cantilever retaining walls. Paper presented at Geotechnics for Sustainable Development - Geotec Hanoi 2013, Hanoi, Vietnam.
Stahl, M., Konietzky, H., 2011. Discrete element simulation of ballast and gravel under special consideration of grain-shape, grain size and relative density, Granular Matter 4: 417-428.
Tuấn, N.Q., Konietzky, H. 2013. DEM simulation of mechanical lab tests for coarse-grained granular material. Paper presented at Geotechnics for Sustainable Development - Geotec Hanoi 2013, Hanoi
Tuấn NQ. 2015. DEM Analysis of fibre-reinforced sand. Paper presented at 10. Freiberg-St.- Petersburger Kolloquium junger Wissenschaftle, Freiberg.
Wang, Y. H., & S. C. Leung, 2008. A particulate-scale investigation of cemented sand behavior. Canadian Geotechnical Journal 45: 29-44.
Yamaguchi T, Maeda K, Matsumoto T, Ibraim E. 2009. 2D DEM analysis on reinforcement effect in granular material using fibre. Journal of Applied Mechanics,JSCE 12: 497-506.